

Resolution and location uncertainties in surface microseismic monitoring

Michael Thornton*, MicroSeismic Inc., Houston, Texas
mthornton@microseismic.com

GeoConvention 2012: Vision

Summary

While related concepts, resolution and uncertainty are distinct. Resolution refers to the size and shape of the focused event image, while location uncertainty describes the effect of noise on the estimates of the image position. Synthetic modeling and comparison to case studies are used to characterize the relationship between the two and to demonstrate that positional uncertainties for surface based monitoring are similar to those for down-hole monitoring, but with a much broader viewing area.

Introduction

Microseismic monitoring can provide important information to help optimize well placement and stimulation programs in unconventional reservoirs (Maxwell, 2010). Surface microseismic monitoring offers several operational advantages over borehole monitoring. Surface arrays do not require dedicated monitoring borehole, and are well disposed for long-term field monitoring. Additionally, the increased distance between event and receiver offers a much larger field of view, allowing long laterals or multi-well pads to be monitored in their entirety (Duncan and Eisner, 2010). Surface deployment of large 2D or 3D arrays captures a large portion of the emitted microseismic wave field, enabling well constrained event imaging with only compressional waves, significantly reducing the sensitivity to velocity model assumptions.

While the surface arrays offer several advantages, there are two main challenges: 1) reduced signal amplitude due to increased distance between event hypocenter and receiver, 2) generally higher levels of noise at surface. While borehole monitoring schemes typically rely on detection of events followed by event location, the reduced signal-to-noise-ratio (SNR) at the surface does not generally allow detection of signals in the unstacked data (e.g., Zhebel et al., 2010). Migration based imaging schemes address this problem by simultaneously improving the SNR through stacking and positioning the events at their proper location. In this approach one must then rely on signal detection after migration which leads to two levels of uncertainty: 1) uncertainty in the detection of signal, 2) uncertainty in the localization of the event.

In this paper, synthetic modeling will be used to illustrate the performance characteristics of the migration process in terms of signal detection and false-alarm rates, along with uncertainties in positional estimates. Examples from two case studies illustrate the magnitude of uncertainties achievable in actual monitoring surveys.

Method

Migration based approach to microseismic imaging involves three steps: downward continuation by beamforming, followed by event detection, then event localization (estimation of event location and timing). Beamforming is accomplished by a progressive scan of potential hypocenter locations in the subsurface. For each potential source location, the data recorded across the array are summed along diffraction curves, forming a beamformed trace, a continuous estimate of the potential source history at the subsurface location over the course of the recording.

As microseismic events are transient events, potential events in the beamformed trace are then identified and extracted. Identification of an event is accomplished via amplitude ratio test. The ratio of RMS amplitude within a sliding event window (the signal estimate) to the RMS amplitude in a trailing window (the noise estimate) is used to compute an estimated SNR. If the SNR exceeds a specified threshold, the event window is marked as a potential trigger.

Once all triggers are detected over all potential hypocenter locations, the catalog is analyzed to localize the event. Due to the finite extent of the array and the restriction of the array to the near surface, the point response of the migration is spread across many subsurface locations. For a surface array with an aperture twice the depth of interest, this point spread function will be elongated in the vertical direction by roughly a factor of three compared to the horizontal response. This elongated shape is primarily due to the trade-off between time of the event (i.e., origin time) and depth of the event when origin time of the event is unknown (Eisner et al., 2009). The actual size of this response is determined by the frequency of the received signal, the velocity of the overburden, distance to the event as well as the array configuration. The localization step consists of identification and evaluation of triggers related to a given event and a secondary diffraction sum along the time/depth trade-off trajectory (Duncan et al., 2010). This secondary diffraction sum, allows one to estimate the timing and location of optimal energy focus and hence the event position.

Uncertainty

Uncertainty in migration based microseismic imaging arises in two primary contexts. First, is uncertainty in the detection step: How certain can we be that the detected events are, in fact, true microseismic events and not spurious noise? The second context relates to the event localization: How accurate are the positional estimates, especially in the vertical direction?

In the case of large events that are visible in the unstacked data, the pattern of moveout and wavelet variation can be readily identified by an experienced analyst as a valid event. However, as one pursues weaker and weaker events, this approach soon fails as the signal disappears into the noise. The statistics of signal detection (McDonough and Whalen, 1995) provides a framework that allows one to provide quantitative estimates of the probability of valid detections along with the probabilities of false alarms. By specifying the detection step as a likelihood ratio test using SNR, it is possible to show that one effectively fixes the probability of false-alarms in the system while maximizing the probability of detection. In general, it is not possible to choose a likelihood ratio test that reduces the probability of false-alarms to zero, so one must accept some probability of false-alarms. In practice, one must balance the false-alarm probability against the probability of failing to detect valid signal.

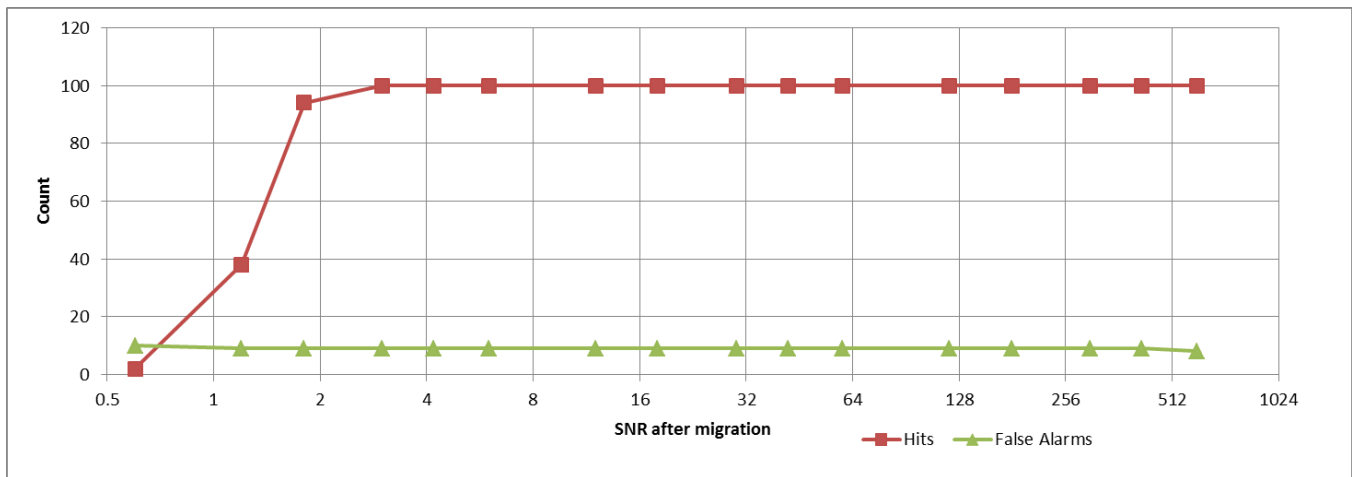


Figure 1: Count of detected events as a function of SNR after migration. Detected events matched to modeled events are shown as hits, events without a match are shown as false alarms.

While it is difficult to assign a certainty to an individual detected event, detection theory does supply some useful insights to the event catalog as a whole. First, we know that the event catalog will contain some percentage of false-alarms. Secondly, theory predicts that the probability of detection should show three distinct zones as a function of SNR. Above some threshold, detection should be nearly certain; below a second threshold, detection should be nearly impossible, and a third relatively narrow transition zone in between.

Estimating an event location ultimately comes down to selection of an optimal focusing point. Uncertainty in this estimate is driven by the effect of noise in this selection process. While the particulars of how noise interacts with the selection process are specific to the selection algorithm, we can predict that noise will tend to move the estimated location along contours of the migration point response and that the impact of noise should decrease with increasing SNR.

Synthetic Modeling

Synthetic modeling is used to assess both types of uncertainty in our imaging algorithm. Synthetic events at known locations were generated and contaminated with varying levels of noise to simulate variable SNR levels. Various array geometries and signal configurations can be simulated, all with similar uncertainty performance characteristics.

Figure 1 shows number of hits and false-alarms for each output SNR level. For SNR > 2, all 100 of the seeded events were detected. For SNR < 2, the detection rate rapidly drops, effectively reaching zero for SNR < 1. This behavior suggests that we can use SNR as an indicator of reliability in the performance in the algorithm. Above some SNR threshold valid events are reliably detected, while below this threshold valid events are missed.

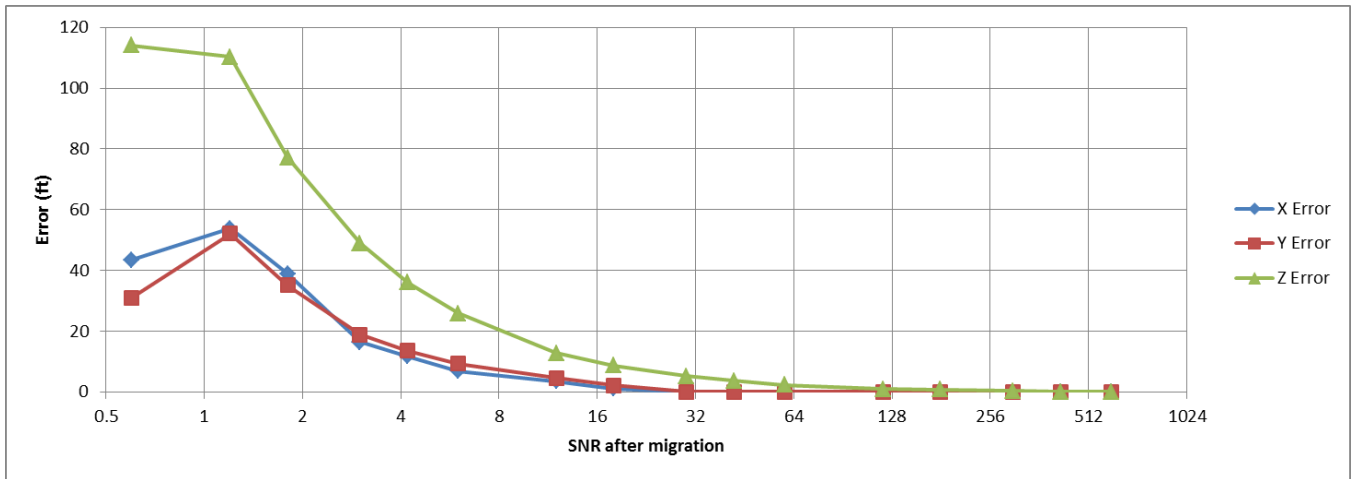


Figure 2: Standard deviation of positional errors as a function of SNR after migration.

Figure 2 shows the standard deviations of positional errors computed from the matched events (hits) shown above. Not shown in the figure are the average errors, for SNR > 1 average errors are very close to zero for all three dimensions indicating the estimates are unbiased. For SNR > 1, we see an exponential decline in variability of the errors, with horizontal and vertical uncertainties converging to near zero for very high SNR values. Variability in X and Y are approximately equal and 2-3 times smaller than variability in Z. The rate of decline in variability in all three dimensions is approximately the same. The estimates with SNR < 1 should be discounted as it contains only 2 hits, and origin time errors associated with these two hits are significantly larger than the other hits (50ms vs. 5ms), indicating these are not likely valid matches.

As predicted, sensitivity to noise in the vertical direction is greater than in the lateral direction. The relative magnitude of the vertical and horizontal sensitivity is roughly proportional to the elongation of the migration point spread response. Furthermore, the impact of noise on the positional estimates diminishes rapidly with increasing SNR.

Case Study	Number of events	Depth Of Target (ft)	SNR Range	Std. Dev. X error (ft)	Std. Dev. Y error (ft)	Std. Dev. Z error (ft)
1	85	7,000	3-10	76	106	116
2	28	11,000	8-30	51	59	52

Table 1: Summary of uncertainty in calibration errors in two case studies.

Case Studies

Table 1 summarizes the analysis of uncertainty in two calibration studies from separate hydraulic fracture monitoring surveys in two different shale plays in North America. Both utilized radial surface arrays consisting of approximately 1000 channels in each. In both cases, perforation shots were used to calibrate the velocity and static corrections for the array. Once the calibration was determined, the imaged positions of the detected perforation shots were compared to the measured location of the gun. The SNR range for the set of shots and the standard deviation of the errors are reported. The estimated uncertainties in positions may be subject to a systematic bias as measured locations of perforation shots can be offset due to errors in deviation surveys (see Bulant et al. 2007).

In Case #1, 85 shots were imaged over a pad of 5 lateral wells. Even though all the shots used similar charges, the SNR range varied from 3 to 10, with 60% of the shots having a SNR < 5. The difference SNR is likely result of variable conversion of charge energy to seismic energy as also observed by Chambers et al. (2010). We consider SNR < 5 to be fairly low SNR for calibration. Average errors in all three dimensions were less than 30 feet.

In Case #2, 28 shots were imaged over a single lateral well. Although the target here was much deeper than the first case, the SNR range is considerably higher, with 78% of the shots having a SNR >15. We consider this to be very good SNR for calibration. Average errors in all three dimensions were less than 20 feet.

While the positional uncertainties in both cases are larger than those shown in the synthetic model, they do show a similar behavior. Case #2 which is characterized by a larger SNR shows a smaller uncertainty indicated by a smaller standard deviation of the errors. Case #2 also shows similar uncertainties in horizontal and vertical directions comparable to the convergence zone noted in the synthetic model. The increased uncertainty compared to the model is likely due to the real-world need to estimate both velocity and static corrections and the presence of coherent noise in real data. In both cases, the uncertainties reported here were deemed acceptable by the operator.

Conclusions

Signal-to-noise-ratio (SNR) is a key indicator of the uncertainty in migration based imaging of microseismic events. Reliability, in terms of the ability to detect the complete set of events is nearly a step-function of SNR. Events with SNR above a threshold of 2-3 are readily detected, while events with SNR below the threshold are missed. Positional uncertainties likewise are driven by SNR. While vertical uncertainty is more sensitive to noise, both horizontal and vertical uncertainties decrease rapidly with increasing SNR. While SNR can be used to infer the relative likelihood that given event is real, false-alarms will occur. Discriminating the real event from the false will require additional information beyond SNR.

While synthetic modeling is useful in assessing the performance characteristic of the imaging method, a number of simplifying assumptions were made that differ from actual application of the method. First, our model assumed that travel-times were known exactly. In practice, velocity and static corrections must be estimated from calibration shots (sources at known locations in the subsurface). While travel time errors are most likely to decrease the SNR after migration, long period errors in travel times could cause spurious focusing and add uncertainty. Secondly, the model assumed the additive noise was Gaussian. While this is a reasonable first approximation, it does not take into account coherent noises, which are ubiquitous in surface microseismic monitoring. Appropriate preprocessing can reduce the impact of coherent noise, but residual coherent noise will trigger false-alarms.

References

Bulant, P., L. Eisner, I. Psencik, and J. L. Calvez, 2007, Importance of borehole deviation surveys for monitoring of hydraulic fracturing treatments: *Geophysical Prospecting*, 55, 891-899.

Chambers, K., S. Brandsberg-Dahl, J.-M. Kendall, and J. Rueda, 2008, Testing the ability of surface arrays to locate microseismicity: 78th Annual International Meeting, SEG, Expanded Abstracts, 1436–1440.

Duncan P., Eisner L., 2010: Reservoir characterization using surface microseismic monitoring. *Geophysics*, 75, pp. 75A139–75A146; doi:10.1190/1.3467760.

Duncan, P.M., J.D. Lakings, and R.A. Flores, 2010, Method for Passive Seismic Emission Tomography: U.S. Patent 7,663,970 B2.

Eisner L., Heigl W.M., Duncan P.M., Keller W.R., 2009: Uncertainties in passive seismic monitoring. *The Leading Edge*; v. 28; no. 6; p. 648-655; DOI: 10.1190/1.3148403.

Maxwell, S., 2010, Microseismic: Growth born from success. *The Leading Edge*, vol. 29, No. 3, p. 338-343.

McDonough, R. N., and A. D. Whalen, 1995, *Detection of signals in noise*. Academic Press, Waltham, MA.

Zhebel, O., Gajewski D., and Venelle C., 2010, *SEG Expanded Abstracts* **29**, 2181-2185.